Reactive processing of formaldehyde and acetaldehyde in aqueous aerosol mimics: Surface tension depression and secondary organic products

Z. Li, A. N. Schwier, N. Sareen, and V. F. McNeill*

Department of Chemical Engineering, Columbia University, New York, NY, 10027

*Correspondence to: V. Faye McNeill (vfm2103@columbia.edu)

Abstract

The reactive uptake of carbonyl-containing volatile organic compounds (cVOCs) by aqueous atmospheric aerosols is a likely source of particulate organic material. The aqueous-phase secondary organic products of some cVOCs are surface-active. Therefore, cVOC uptake can lead to organic film formation at the gas-aerosol interface and changes in aerosol surface tension. We examined the chemical reactions of two abundant cVOCs, formaldehyde and acetaldehyde, in water and aqueous ammonium sulfate (AS) solutions mimicking tropospheric aerosols. Secondary organic products were identified using Aerosol Chemical Ionization Mass Spectrometry (Aerosol-CIMS), and changes in surface tension were monitored using pendant drop tensiometry. Hemiacetal oligomers and aldol condensation products were identified using Aerosol-CIMS. A hemiacetal sulfate ester was tentatively identified in the formaldehyde-AS system. Acetaldehyde depresses surface tension to $65(\pm2)$ dyn cm^{-1} in pure water and $62(\pm1)$ dyn cm^{-1} in AS solutions. Surface tension depression by formaldehyde in pure water is negligible; in AS solutions, a 9% reduction in surface tension is observed. Mixtures of these species were also studied in combination with methylglyoxal in order to evaluate the influence of cross-reactions on surface tension depression and product formation in these systems. We find that surface tension depression in the solutions containing mixed cVOCs exceeds that predicted by an additive model based on the single-species isotherms.

1 Introduction

Organic material is a ubiquitous component of atmospheric aerosols, making up a major fraction of fine aerosol mass, but its sources and influence on aerosol properties are still poorly constrained (Kanakidou et al., 2005; Jimenez et al., 2009). Many common organic aerosol species are surface-active (Shulman et al., 1996; Facchini et al., 1999). Surface-active molecules in aqueous solution form structures that allow hydrophobic groups to avoid contact with water while hydrophilic groups remain in solution. In an aqueous aerosol particle, they may partition to the gas-aerosol interface, reducing aerosol surface tension and potentially acting as a barrier to gas-aerosol mass transport (Folkers et al., 2003; McNeill et al., 2006). Depressed aerosol surface tension due to film formation may lead to a decrease in the critical supersaturation required for the particle to activate and grow into a cloud droplet as described by Köhler Theory (Kohler, 1936). The surface tension of atmospheric aerosol samples tends to be lower than that predicted based on the combined effects of the individual surfactants identified in the aerosol (Facchini et al., 1999). This is in part because some surface-active aerosol organics remain unidentified. Additionally, the effects of interactions among these species under typical aerosol conditions (i.e. supersaturated salt concentrations, acidic, multiple organic species) are generally unknown.

The adsorption of volatile organic compounds (VOCs) to aqueous aerosol and cloud droplet surfaces has been proposed as a route for the formation of organic surface films (Djikaev and Tabazadeh, 2003; Donaldson and Vaida, 2006). There is also growing evidence that the reactive uptake of the carbonyl-containing VOCs (cVOCs) methylglyoxal and glyoxal by cloud droplets or aerosol water, followed by aqueous-phase chemistry to form low-volatility products, is a source of secondary aerosol material (Ervens and Volkamer, 2010; Lim et al., 2010). We recently showed that methylglyoxal suppresses surface tension in aqueous aerosol mimics (Sareen et al., 2010).

Formaldehyde and acetaldehyde, two abundant, highly volatile aldehydes, can be directly emitted from combustion and industrial sources or generated *in situ* via the

oxidation of other VOCs (Seinfeld and Pandis, 1998). In aqueous solution, both for-
maldehyde and acetaldehyde become hydrated and form acetal oligomers, similar to
methylglyoxal and glyoxal (Loudon, 2009). Nozière and coworkers showed that acet-
aldehyde forms light-absorbing aldol condensation products in aqueous ammonium
sulfate solutions (Nozière et al., 2010a). Formaldehyde was also recently suggested to
react with amines to form organic salts in tropospheric aerosols (Wang et al., 2010).
Due to their prevalence and known aqueous-phase oligomerization chemistry, the re-
active processing of these species in aqueous aerosol mimics, alone and in combina-
tion with other cVOCs, is of interest, but has not been thoroughly studied to date.

We investigated the chemical reactions of formaldehyde and acetaldehyde in pure
water and concentrated ammonium sulfate (AS) solutions mimicking aerosol water.
The potential of these species to alter aerosol surface tension was examined, and sec-
ondary organic products were identified using Aerosol Chemical Ionization Mass
Spectrometry (Aerosol-CIMS).

2   Experimental Methods

Aqueous solutions containing varying concentrations of organic compounds (ac-
etaldehyde, formaldehyde and/or methylglyoxal) with near-saturation concentrations
(3.1 M) of AS were prepared in 100 mL Pyrex vessels using Millipore water. The
concentration of acetaldehyde was 0.018 M – 0.54 M. In the preparations, 5 mL am-
pules of 99.9 wt% acetaldehyde (Sigma Aldrich) were diluted to 1.78 M using Milli-
pore water immediately after opening in order to minimize oxidization. Varying
amounts of this stock solution were used to prepare the final solutions within 30
minutes of opening the ampule. Formaldehyde and methylglyoxal (MG) were intro-
duced from 37 wt% and 40 wt% aqueous solutions (Sigma Aldrich), respectively. The
pH value of the reaction mixtures, measured using a digital pH meter (Accumet, Fish-
er Scientific), was 2.7-3.1.

The surface tension of each sample was measured 24 hours after solution prepara-
tion using pendant drop tensiometry (PDT). Pendant drops were suspended from the

83   tip of glass capillary tubes using a 100 μL syringe. The images of the pendant drops

84   were captured and analyzed to determine the shape factor, H, and equatorial diameter,

85   d_e, as described previously (Sareen et al., 2010; Schwier et al., 2010). These parame-

86   ters were used to calculate the surface tension according to:

87    $$\sigma = \frac{\Delta \rho g d_e^2}{H} \tag{1}$$

88   where σ is surface tension, $\Delta \rho$ is the difference in density between the solution and the

89   gas phase, and g is acceleration due to gravity (Adamson and Gast, 1997). Solution

90   density was measured using an analytical balance (Denver Instruments). The drops

91   were allowed to equilibrate for 2 minutes before image capture. Each measurement

92   was repeated 7 times.

93   Aerosol-CIMS was used to detect the organic composition of the product mix-

94   tures as described in detail previously (Sareen et al., 2010; Schwier et al., 2010). Mix-

95   tures of formaldehyde, acetaldehyde-MG, and formaldehyde-MG in water and 3.1 M

96   AS were prepared. Total organic concentration ranged from 0.2-2 M. All the AS solu-

97   tions were diluted at 24 hours with Millipore water until the salt concentration was 0.2

98   M. The solutions were aerosolized in a stream of N_2 using a constant output atomizer

99   (TSI) and flowed through a heated 23 cm long, 1.25 cm ID PTFE tube (maintained at

100   135°C) at RH >50% before entering the CIMS, in order to volatilize the organic spe-

101   cies into the gas phase for detection. The time between atomization and volatilization

102   (≤ 3.5 s) is too short for detectable quantities of the expected reaction products to

103   form, therefore the detected molecules are most likely formed in the bulk aqueous so-

104   lutions. The solutions were tested in both positive and negative ion mode, using

105    $H_3O^+ \cdot (H_2O)_n$ and I^- as reagent ions, respectively. The applicability of this approach to

106   the detection of acetal oligomers and aldol condensation products formed by dicar-

107   bonyls in aqueous aerosol mimics has been demonstrated previously (Sareen et al.,

108   2010; Schwier et al., 2010). The average particle concentration was ~4×10^4 cm^{-3} and

109   the volume weighted geometric mean diameter was 414($\pm$14) nm.

110   The Pyrex vessels shielded the reaction mixtures from UV light with wavelengths

111   < 280 nm (Corning, Inc.), but the samples were not further protected from visible

112   light. We previously showed that exposure to visible light in identical vessels does not

113   impact chemistry in the glyoxal-AS or MG-AS reactive systems (Sareen et al., 2010;

114   Shapiro et al., 2009).

3   Results

3.1 Surface Tension Measurements

117   **3.1.1**   **Single-organic mixtures**. Results of the PDT experiments (Fig. 1) show that

118   both formaldehyde and acetaldehyde depress surface tension in 3.1 M AS solution,

119   but the formaldehyde mixture is less surface-active than that of acetaldehyde. The

120   formaldehyde-AS solutions reach a minimum surface tension of 71.4 ± 0.4 dyn cm^{-1} at

121   0.082 mol C/kg H_2O. This represents a 9% reduction in surface tension from that of a

122   3.1 M AS solution (78.5 ± 0.3 dyn cm^{-1}). The acetaldehyde-AS solutions showed more

123   significant surface tension depression. The surface tension of the solutions reached a

124   minimum of 62 ± 1 dyn cm^{-1} when the acetaldehyde concentration exceeded 0.527 mol

125   C/kg H_2O (20.6% reduction compared to 3.1 M AS solution). Compared to the surface

126   tension of the acetaldehyde in 3.1 M AS, the surface tension depression of acetalde-

127   hyde in water is less significant. The surface tension of acetaldehyde in water de-

128   creases rapidly and reaches a minimum value of 65 ± 2 dyn cm^{-1} at 0.89 mol C/kg H_2O.

129   Formaldehyde does not show any detectable surface tension depression in water in the

130   absence of AS.

131   The surface tension data can be fit using the Szyszkowski-Langmuir equation:

132   $$\sigma = \sigma_0 - aT\ln(1 + bC) \qquad\qquad (2)$$

133   where σ and σ_0 are surface tension of the solution with and without organics, T is am-

134   bient temperature (298 K), C is total organic concentration (moles carbon per kg

135   H_2O), and a and b are fit parameters (Adamson and Gast, 1997). The parameters from

136   the fits to the data in Fig. 1 are listed in Table 1.

137   **3.1.2**   **Binary mixtures.** Surface tension results for aqueous solutions containing a

138   mixture of two organic compounds (MG and formaldehyde or acetaldehyde) and 3.1

139 M AS are shown in Fig. 2. For a given total organic concentration (0.5 or 0.05 M), the

140 surface tension decreased with increasing MG concentration. Re-plotting the data

141 from Fig. 2 as a function of MG concentration, it is apparent that the surface tension

142 was very similar for mixtures with the same MG concentration, regardless of the iden-

143 tity or amount of the other species present in the mixture (Fig. 3).

144 Henning and coworkers developed the following model based on the Szyszkow-

145 ski-Langmuir equation to predict the surface tension of complex, nonreacting mix-

146 tures of organics (Henning et al., 2005):

147 $$\sigma = \sigma_0(T) - \sum_i \chi_i a_i T \ln(1 + b_i C_i) \tag{3}$$

148 Here, C_i is the concentration of each organic species (moles carbon per kg H_2O), χ_i is

149 the concentration (moles carbon per kg H_2O) of compound i divided by the total solu-

150 ble carbon concentration in solution, and a_i and b_i are the fit parameters from the

151 Szyszkowski-Langmuir equation for compound i. The Henning model has been

152 shown to describe mixtures of nonreactive organics, such as succinic acid-adipic acid

153 in inorganic salt solution, well (Henning et al., 2005). We also found that it was capa-

154 ble of describing surface tension depression in reactive aqueous mixtures containing

155 MG, glyoxal, and AS (Schwier et al., 2010).

156 The predicted surface tension depression for the binary mixtures as calculated

157 with the Henning model is shown in Fig. 2 as a black line, and the confidence inter-

158 vals based on uncertainty in the Szyszkowski-Langmuir parameters are shown in grey.

159 The experimentally measured surface tensions are, in general, lower than the Henning

160 model prediction, indicating a synergistic effect between MG and acetalde-

161 hyde/formaldehyde. The error of the prediction for the mixtures of MG and acetalde-

162 hyde is between 8-24%. The error tends to increase with the concentration of MG.

163 However, the error is less than 10% for formaldehyde-MG mixtures.

164 **3.1.3   Ternary mixtures.** As shown in Fig. 4, 3.1 M AS solutions containing ter-

165 nary mixtures of MG, acetaldehyde and formaldehyde also exhibit surface tension de-

166 pression lower than that predicted by the Henning model. For the ternary mixture ex-

167 periments, the molar ratio of acetaldehyde to formaldehyde was either 1:3 (Fig. 4a

168 and 4b) or 1:1 (Fig. 4c and 4d) and the MG concentration was varied. The total organ-

169 ic concentration remained constant at 0.05 M. Recasting the data of Fig. 4 as a func-

170 tion of MG concentration shows a similar trend as what was observed for the binary

171 mixtures; for a constant total organic concentration, MG content largely determines

172 the surface tension, regardless of the relative amounts of acetaldehyde and formalde-

173 hyde present (Fig. 3).

174

175 **3.2 Aerosol-CIMS characterization**

176 The CIMS data show products of self- and cross-reactions of formaldehyde, acetalde-

177 hyde and MG in pure water and 3.1 M AS. We did not perform Aerosol-CIMS analy-

178 sis on acetaldehyde-AS or acetaldehyde-H_2O solutions because these systems have

179 been characterized extensively by others (Nozière et al., 2010a; Casale et al., 2007).

180 **3.2.1   Formaldehyde.** The mass spectra for formaldehyde in H_2O and in 3.1 M AS

181 obtained using negative ion detection with I^- as the reagent ion is shown in Fig. 5.

182 Possible structures are shown in Table 2. The spectrum shows peaks with mass-to-

183 charge ratios corresponding to formic acid at 81.7 ($CHO_2^-\cdot 2H_2O$) and 208.7 amu (I^-

184 $\cdot CH_2O_2\cdot 2H_2O$) and several peaks consistent with hemiacetal oligomers. 223.3, 291.1,

185 and 323.5 amu are consistent with clusters of hemiacetals with I^-. A small amount of

186 formic acid impurity exists in the 37% formaldehyde aqueous stock solution (Sigma

187 Aldrich). The peaks at 95.6, 110.4, 273.8 and 304.7 amu are consistent with clusters

188 of ionized hemiacetals with H_2O. While ionization of alcohols by I^- is normally not

189 favorable, ionized paraformaldehyde-type hemiacetals are stabilized by interactions

190 between the ionized $-O^-$ and the other terminal hydroxyl group(s) on the molecule

191 (see the Supporting Information).

192 Within our instrument resolution, the peaks at m/z 176.7 and 193.8 amu peaks could

193 be consistent with the mass of methanol, which is added to commercial formaldehyde

194 solutions as a stabilizer. However, methanol is not predicted to cluster with I^-. Fur-

195 thermore, these peaks are not observed in the formaldehyde-H_2O spectrum and are

196 present only with the addition of AS, implying that the species observed at those

8

masses are formed via reaction with AS. No favorable pathway for the reduction of formaldehyde to form methanol in an acidic medium is known. The peak at 193.8 amu is consistent with an organosulfate species formed from a formaldehyde hemiacetal dimer ($C_2H_5O_6S^- \cdot 2H_2O$). The peak at 176.7 amu matches an ion formula of $C_6H_9O_6^-$ or $C_2H_7O_6S^- \cdot H_2O$, but the structures and formation mechanisms of those species are unknown.

The positive-ion spectrum of the formaldehyde solution in 3.1 M AS corroborates the identification of hemiacetal oligomers. To our knowledge, organosulfate species have not previously been observed using proton-transfer mass spectrometry (Sareen et al., 2010). The spectrum and peak assignments can be found in the Supporting Information.

3.2.2   Formaldehyde-methylglyoxal mixtures. The negative-ion spectrum (detected with I^-) for an aqueous mixture of formaldehyde, MG, and AS is shown in Fig. 6, with possible peak assignments listed in Table 3. Most of the peaks are consistent with formaldehyde hemiacetal oligomers, such as 186.7, 203.5, 230.3, 257.4, and 264.5 amu. Formic acid was detected at 172.8 amu and 208.7 amu. The peak at 288.1 corresponds to MG self-reaction products formed either via aldol condensation or hemiacetal mechanisms (Sareen et al., 2010; Schwier et al., 2010). Several peaks could correspond to self-reaction products of either formaldehyde or MG: 216.5, 252.4, 324.5, and 342.6 amu. The peak at 314.3 amu is consistent with a hemiacetal oligomer formed via cross-reaction of MG with two formaldehyde molecules, clustered with I^- and two water molecules. The peak at 272.2 amu could correspond to either a similar cross-reaction product (MG + 2 formaldehyde) or a MG dimer. Formaldehyde hemiacetal self-reaction products and formic acid were detected in the positive-ion spectrum (Supporting Information).

3.2.3   Acetaldehyde-methylglyoxal mixtures. The $H_3O^+(H_2O)_n$ spectrum for aqueous acetaldehyde-MG-AS mixtures is shown in Figure 7, with peak assignments listed in Table 4. Hydrated acetaldehyde can be observed at 98.4 amu. Several peaks are consistent with the cross-reaction products of MG and acetaldehyde via an aldol

9

226   mechanism (126.0, 134.0, 206.7, and 248.9 amu). Formic, glyoxylic, and glycolic ac-

227   ids correspond to the peaks at 84.4, 93.5, and 95.5 amu, respectively. Since no signifi-

228   cant source of oxidants exists in the reaction mixtures, the formation mechanisms for

229   these species in this system are unknown. The peaks at 88.9 and 107.2 are consistent

230   with either pyruvic acid or crotonaldehyde. Large aldol condensation products from

231   the addition of 6-10 acetaldehydes are observed at 192.9, 289.6, and 297 amu. The

232   peaks at 145.1, 162.9, 164.7 and 235 amu are consistent with MG self-reactions, as

233   discussed by Sareen et al (2010). The peak at 137.3 amu is consistent with a species

234   with molecular formula $C_5H_{12}O_3$, but the mechanism is unknown.

235   The I^- negative-ion spectrum for acetaldehyde-MG-AS mixtures shows similar

236   results to the positive-ion spectrum (see Figure 8 and Table 5), however aldol conden-

237   sation products are not detected by this method unless they contain a terminal carbox-

238   ylic acid group or neighboring hydroxyl groups (Sareen et al., 2010). Small acid spe-

239   cies, such as formic, acetic and crotonic acid (172.7 (208.4), 186.4 and 230.7 amu,

240   respectively), were detected. Hydrated acetaldehyde (189.6 and 224.1 amu) and MG

241   (216.3 amu), and hemiacetal self-dimers of acetaldehyde and MG (230.7, 256.4,

242   264.4, 269.5, and 342.3) were also observed. 256.4 amu is consistent with a MG aldol

243   condensation dimer product, and 272.2 amu could correspond either to a MG hemiac-

244   etal dimer or an aldol condensation product. 242.9 amu, $I^-·C_5H_8O_3$, is consistent with

245   an aldol condensation cross product of MG and acetaldehyde. 194.6 amu corresponds

246   to both of the following ion formulas, $C_6H_9O_6^-$ and $C_2H_7O_6S^-·H_2O$, but the mecha-

247   nisms and structures are unknown.

248   Note that several peaks appear at similar mass-to-charge ratios in the negative

249   mode mass spectra of both the formaldehyde-MG and acetaldehyde-MG mixtures.

250   MG self-reaction products are expected to be present in both systems. Beyond this,

251   formaldehyde and acetaldehyde are structurally similar small molecules which follow

252   similar oligomerization mechanisms alone and with MG. In several cases, peaks in the

253   mass spectra corresponding to structurally distinct expected reaction products for each

254   system have similar mass-to-charge ratios. For example, the formaldehyde hemiacetal

255   4-mer ($I^-C_4H_{10}O_5$) and the acetaldehyde dimer ($I^-C_4H_6O_3 \cdot 2H_2O$) are both apparent at

256   264 amu.

4. Discussion

258   Both formaldehyde and acetaldehyde, and their aqueous-phase reaction products,

259   were found to depress surface tension in AS solutions. However, surface tension de-

260   pression was not observed in aqueous formaldehyde solutions containing no salt. Net

261   surface tension depression by acetaldehyde was greater in the AS solutions than in

262   pure water. These differences are likely due to chemical and physical effects of the

263   salt. The salt promotes the formation of surface-active species: several of the reaction

264   products in the AS systems identified using Aerosol-CIMS are known or expected to

265   be surface-active, such as organosulfates (Nozière et al., 2010b) and organic acids.

266   Salts can also alter the partitioning of these volatile yet water-soluble organic species

267   between the gas phase and aqueous solution. Formaldehyde has a small Henry's Law

268   constant of 2.5 M atm^{-1}, although hydration in the aqueous phase leads to an effective

269   Henry's Law constant of 3×10^3 M atm^{-1}, similar to that of MG (Seinfeld and Pandis,

270   1998; Betterton and Hoffmann, 1988). The effective Henry's Law constant for acetal-

271   dehyde in water at 25°C was measured by Betterton and Hoffmann (1988) to be 11.4

272   M atm^{-1}. The Henry's Law constant of formaldehyde was shown by Zhou and Mopper

273   to increase slightly in aqueous solutions containing an increasing proportion of sea-

274   water (up to 100%), but the opposite is true for acetaldehyde (Zhou and Mopper,

275   1990). The reaction mixtures studied here equilibrated with the gas phase for 24 h be-

276   fore the surface tension measurements were performed. Each pendant drop equilibrat-

277   ed for 2 min before image capture, after which time there was no detectable change in

278   drop shape. Some of the organics may be lost to the gas phase during equilibration.

279   However, the lower volatility of the aqueous-phase reaction products, especially those

280   formed through oligomerization, leads to significant organic material remaining in the

281   condensed phase (enough to cause surface tension depression and be detected via

282   Aerosol-CIMS).

283   When formaldehyde and acetaldehyde are present in combination with MG, as

284   would likely happen in the atmosphere, there is a synergistic effect: surface tension

285   depression in the solutions containing mixed organics exceeds that predicted by an

286   additive model based on the single-species isotherms. This effect could be due to the

287   formation of more surface-active reaction products in the mixed systems. The devia-

288   tion from the Henning model prediction was less than 10% except in the case of the

289   acetaldehyde-MG-AS mixtures. Between 21-30% of the detected product mass was

290   identified as cross products in the Aerosol-CIMS positive mode analysis of the acetal-

291   dehyde-MG mixtures following Schwier et al. (2010). Most of the oligomers identi-

292   fied in this system were aldol condensation products, which have fewer hydroxyl

293   groups than acetal oligomers and are therefore expected to be more hydrophobic. A

294   number of organic acid products, likely to be surface-active, were also identified in

295   the acetaldehyde-MG-AS system.

296   In contrast to the MG-glyoxal system (Schwier et al., 2010), the presence of for-

297   maldehyde and/or acetaldehyde in aqueous MG-AS solutions does influence surface

298   tension depression, in fact, to a greater extent than predicted by the Henning model.

299   However, the results of the binary and ternary mixture experiments suggest that MG

300   still plays a dominant role in these systems since the measured surface tension was

301   remarkably similar in each mixture for a given MG concentration.

302   The formaldehyde hemiacetal dimer ($C_2H_6O_6S$) may form via the reaction of

303    $C_2H_6O_3$ with H_2SO_4 (Deno and Newman, 1950). The equilibrium concentration of

304   H_2SO_4 in our bulk solutions (3.1 M AS, pH = 3) is small (2.8×10^{-7} M). Minerath and

305   coworkers showed that alcohol sulfate ester formation is slow under tropospheric aer-

306   osol conditions (Minerath et al., 2008). Based on our observations, assuming a maxi-

307   mum Aerosol-CIMS sensitivity of 100 Hz ppt^{-1} to this species (Sareen et al., 2010) we

308   infer a concentration of $\geq 2 \times 10^{-4}$ M in the bulk solution after 24 h of reaction. Using

309   our experimental conditions and the kinetics of ethylene glycol sulfate esterification

310   from Minerath et al., we predict a maximum concentration of 7×10^{-8} M. This suggests

311   that either a) the kinetics of sulfate esterification for paraformaldehyde are significant-

312 ly faster than for alcohols b) SO_4^{-2} or HSO_4^- is the active reactant, contrary to the con-

313 clusions of Deno and Newman, or c) sulfate esterification is enhanced by atomization.

314 See the Supporting Information for details of these calculations. Photochemical pro-

315 duction of organosulfates has also been observed (Galloway et al., 2009; Nozière et

316 al., 2010b; Perri et al., 2010). Our samples were protected from UV light by the Pyrex

317 reaction vessels, and no significant OH source was present, so we don't expect photo-

318 chemical organosulfate production to be efficient in this system.

319 Nitrogen-containing compounds could also be formed in these reaction mixtures

320 due to the presence of the ammonium ion (Sareen et al., 2010; Nozière et al., 2009;

321 Galloway et al., 2009). No unambiguous identifications of C-N containing products

322 were made in this study, but analysis using a mass spectrometry technique with higher

323 mass resolution could reveal their presence.

324 The relatively low solubility of formaldehyde and acetaldehyde in water suggests

325 that their potential to contribute to total SOA mass is low as compared to highly solu-

326 ble species such as glyoxal. This is supported by the observations of Kroll et al.

327 (2005) that AS aerosols exposed to formaldehyde in an aerosol reaction chamber did

328 not result in significant particle volume growth. However, formaldehyde and acetal-

329 dehyde in the gas phase could adsorb at the aerosol surface (vs. bulk aqueous absorp-

330 tion), and this may also impact aerosol surface tension (Donaldson and Vaida, 2006).

331 Furthermore, Romakkaniemi and coworkers recently showed significant enhancement

332 of aqueous-phase SOA production by surface-active species beyond what would be

333 predicted based on Henry's Law due to surface-bulk partitioning (Romakkaniemi et

334 al., 2011).

335 **5. Conclusions**

336 Two highly volatile organic compounds, formaldehyde and acetaldehyde, were found

337 to form secondary organic products in aqueous ammonium sulfate (AS) solutions

338 mimicking tropospheric aerosols. These species, and their aqueous-phase reaction

339 products, lead to depressed surface tension in the aqueous solutions. This adds to the

340 growing body of evidence that VOCs are a secondary source of surface-active organic

341 material in aerosols.

342

Acknowledgement

348

References

350 Adamson, A. W. and Gast, A. P., Physical chemistry of surfaces, Wiley, New York,
351   1997.

352 Betterton, E. A. and Hoffmann, M. R.: Henry Law Constants of Some Environmental-
353   ly Important Aldehydes, *Environ. Sci. Technol.*, *22* (12), 1415-1418, 1988.

354 Casale, M. T., Richman, A. R., Elrod, M. J., Garland, R. M., Beaver, M. R., and Tol-
355   bert, M. A.: Kinetics of acid-catalyzed aldol condensation reactions of aliphat-
356   ic aldehydes, *Atmos. Environ.*, *41* (29), 6212-6224, 2007.

357 Deno, N. C. and Newman, M. S.: Mechanism of Sulfation of Alcohols, *J. Am. Chem.*
358   *Soc.*, *72* (9), 3852-3856, 1950.

359 Djikaev, Y. S. and Tabazadeh, A.: Effect of adsorption on the uptake of organic trace
360   gas by cloud droplets, *J. Geophys. Res.-Atmos.*, *108* (D22), 4869,
361   doi:10.1029/2003JD003741, 2003.

362 Donaldson, D. J. and Vaida, V.: The influence of organic films at the air-aqueous
363   boundary on atmospheric processes, *Chem. Rev.*, *106* (4), 1445-1461, 2006.

364 Ervens, B. and Volkamer, R.: Glyoxal processing by aerosol multiphase chemistry:
365   Towards a kinetic modeling framework of secondary organic aerosol for-
366   mation in aqueous particles, *Atmos. Chem. Phys.*, *10,* 8219-8244, 2010.

367 Facchini, M. C., Mircea, M., Fuzzi, S., and Charlson, R. J.: Cloud albedo enhance-
368   ment by surface-active organic solutes in growing droplets, *Nature, 401*
369   (6750), 257-259, 1999.

370 Folkers, M., Mentel, T. F., and Wahner, A.: Influence of an organic coating on the re-

371   activity of aqueous aerosols probed by the heterogeneous hydrolysis of N2O5,
372   *Geophys. Res. Lett.*, *30* (12), 1644-1647, doi:10.1029/2003GL017168, 2003.

373   Galloway, M. M., Chhabra, P. S., Chan, A. W. H., Surratt, J. D., Flagan, R. C., Sein-
374   feld, J. H., and Keutsch, F. N.: Glyoxal uptake on ammonium sulphate seed
375   aerosol: reaction products and reversibility of uptake under dark and irradiated
376   conditions, *Atmos. Chem. Phys.*, *9*, 3331-3345, 2009.

377   Henning, S., Rosenorn, T., D'Anna, B., Gola, A. A., Svenningsson, B., and Bilde, M.:
378   Cloud droplet activation and surface tension of mixtures of slightly soluble or-
379   ganics and inorganic salt, *Atmos. Chem. Phys.*, *5*, 575-582, 2005.

380   Jimenez, J. L., et al..: Evolution of Organic Aerosols in the Atmosphere, *Science*, *326*
381   (5959), 1525-1529, 2009.

382   Kanakidou, M., et al.: Organic aerosol and global climate modelling: A review, *Atmos.*
383   *Chem. Phys.*, *5*, 1053-1123, 2005.

384   Kohler, H.: The nucleus in the growth of hygroscopic droplets, *Trans. Faraday Soc.*,
385   *32,* 1152-1161, 1936.

386   Kroll, J. H., Ng, N. L., Murphy, S. M., Varutbangkul, V., Flagan, R. C., and Seinfeld,
387   J. H.: Chamber studies of secondary organic aerosol growth by reactive uptake
388   of simple carbonyl compounds, *J. Geophys. Res.-Atmos.*, *110* (D23), D23207-
389   doi:10.1029/2005JD006004, 2005.

390   Lim, Y. B., Tan, Y., Perri, M. J., Seitzinger, S. P., and Turpin, B. J.: Aqueous chemistry
391   and its role in secondary organic aerosol (SOA) formation, *Atmos. Chem.*
392   *Phys.* , *10* (21), 10521-10539, 2010.

393   Loudon, G. M., Organic chemistry, Roberts and Co., Greenwood Village, CO, 2009.

394   McNeill, V. F., Patterson, J., Wolfe, G. M., and Thornton, J. A.: The effect of varying
395   levels of surfactant on the reactive uptake of N2O5 to aqueous aerosol, *Atmos.*
396   *Chem. Phys.*, *6*, 1635-1644, 2006.

397   Minerath, E. C., Casale, M. T., and Elrod, M. J.: Kinetics feasibility study of alcohol
398   sulfate esterification reactions in tropospheric aerosols, *Environ. Sci. Technol.*,
399   *42* (12), 4410-4415, 2008.

400   Nozière, B., Dziedzic, P., and Cordova, A.: Products and Kinetics of the Liquid-Phase
401   Reaction of Glyoxal Catalyzed by Ammonium Ions (NH4+), *J. Phys. Chem. A*,
402   *113* (1), 231-237, 2009.

403   Nozière, B., Dziedzic, P., and Cordova, A.: Inorganic ammonium salts and carbonate
404   salts are efficient catalysts for aldol condensation in atmospheric aerosols,
405   *Phys. Chem. Chem. Phys.*, *12* (15), 3864-3872, 2010a.

406 Nozière, B., Ekstrom, S., Alsberg, T., and Holmstrom, S.: Radical-initiated formation
407   of organosulfates and surfactants in atmospheric aerosols, *Geophys. Res. Lett.*,
408   *37,* L05806, doi:10.1029/2009GL041683, 2010b.

409 Perri, M. J., Lim, Y. B., Seitzinger, S. P., and Turpin, B. J.: Organosulfates from gly-
410   colaldehyde in aqueous aerosols and clouds: Laboratory studies, *Atmos. Envi-*
411   *ron.*, *44* (21-22), 2658-2664, 2010.

412 Romakkaniemi, S., Kokkola, H., Smith, J. N., Prisle, N. L., Schwier, A. N., McNeill,
413   V. F., and Laaksonen, A.: Partitioning of Semivolatile Surface-Active Com-
414   pounds Between Bulk, Surface, and Gas-Phase, *Geophys. Res. Lett.*, *38* (3),
415   L03807-doi:10.1029/2010GL046147, 2011.

416 Sareen, N., Schwier, A. N., Shapiro, E. L., Mitroo, D. M., and McNeill, V. F.: Second-
417   ary organic material formed by methylglyoxal in aqueous aerosol mimics, *At-*
418   *mos. Chem. Phys.*, *10*, 997-1016, 2010.

419 Schwier, A. N., Sareen, N., Mitroo, D. M., Shapiro, E. L., and McNeill, V. F.: Glyox-
420   al-Methylglyoxal Cross-Reactions in Secondary Organic Aerosol Formation,
421   *Environ. Sci. Technol.*, *44* (16), 6174-6182, 2010.

422 Seinfeld, J. H. and Pandis, S. N., Atmospheric Chemistry and Physics: From air pollu-
423   tion to climate change, Wiley, New York, 1998.

424 Shapiro, E. L., Szprengiel, J., Sareen, N., Jen, C. N., Giordano, M. R., and McNeill, V.
425   F.: Light-absorbing secondary organic material formed by glyoxal in aqueous
426   aerosol mimics, *Atmos. Chem. Phys.* , *9* (7), 2289-2300, 2009.

427 Shulman, M. L., Jacobson, M. C., Carlson, R. J., Synovec, R. E., and Young, T. E.:
428   Dissolution behavior and surface tension effects of organic compounds in nu-
429   cleating cloud droplets, *Geophys. Res. Lett.*, *23* (3), 277-280, 1996.

430 Wang, X. F., Gao, S., Yang, X., Chen, H., Chen, J. M., Zhuang, G. S., Surratt, J. D.,
431   Chan, M. N., and Seinfeld, J. H.: Evidence for High Molecular Weight Nitro-
432   gen-Containing Organic Salts in Urban Aerosols, *Environ. Sci. Technol.*, *44*
433   (12), 4441-4446, 2010.

434 Zhou, X. L. and Mopper, K.: Apparent Partition-Coefficients of 15 Carbonyl-
435   Compounds Between Air and Seawater and Between Air and Fresh-Water -
436   Implications for Air Sea Exchange, *Environ. Sci. Technol.*, *24* (12), 1864-
437   1869, 1990.

438

439

440 **Table 1.** Szyszkowski-Langmuir Fit Parameters according to Eq. (2)

Mixture	σ_0 (dyn cm^{-1})	a (dyn cm^{-1} K^{-1})	b (kg H$_2$O (mol C)$^{-1}$)
Methylglyoxal + 3.1 M (NH$_4$)$_2$SO$_4$ (Sareen et al. 2010)	78.5	0.0185±0.0008	140±34
Acetaldehyde + 3.1 M (NH$_4$)$_2$SO$_4$	78.5	0.0008±0.0046	9.53±3.86
Formaldehyde + 3.1 M (NH$_4$)$_2$SO$_4$	78.5	0.0119±0.0043	50.23±44.8
Acetaldehyde + H$_2$O	72.0	0.0037±0.0011	491.64±689

441

442

443 **Table 2.** Proposed peak assignments for Aerosol-CIMS mass spectra with I$^-$ of atom-
444 ized solutions of 0.2 M formaldehyde in 3.1 M AS.

m/z (amu) ± 1.0 amu	Ion Formula	Molecular Formula	Possible Structures	Mechanism
81.7	CHO$_2^-$·2H$_2$O	CH$_2$O$_2$		Formic Acid
95.6	C$_2$H$_5$O$_3^-$·H$_2$O	C$_2$H$_6$O$_3$		n=2 hemiacetal
110.4	C$_2$H$_3$O$_3^-$·2H$_2$O	C$_2$H$_4$O$_3$		n=2 hemiacetal
176.7	C$_6$H$_9$O$_6^-$ C$_2$H$_7$O$_6$S$^-$·H$_2$O	C$_6$H$_{10}$O$_6$ C$_2$H$_8$O$_6$S	Unknown	Unknown
193.8	C$_2$H$_5$O$_6$S$^-$·2H$_2$O	C$_2$H$_6$O$_6$S		Hemiacetal sulfate
208.7	I$^-$·CH$_2$O$_2$·2H$_2$O	CH$_2$O$_2$		Formic Acid
223.3	I$^-$·C$_2$H$_6$O$_3$·H$_2$O	C$_2$H$_6$O$_3$		n=2 hemiacetal
273.8	C$_8$H$_{15}$O$_9^-$·H$_2$O C$_8$H$_{17}$O$_{10}^-$	C$_8$H$_{16}$O$_9$ C$_8$H$_{18}$O$_{10}$		n=8 hemiacetal
291.1	I$^-$·C$_5$H$_8$O$_6$	C$_5$H$_8$O$_6$		n=5 hemiacetal
304.7	C$_9$H$_{19}$O$_{10}^-$·H$_2$O	C$_9$H$_{20}$O$_{10}$		n=9 hemiacetal
323.5	I$^-$·C$_6$H$_{14}$O$_7$	C$_6$H$_{14}$O$_7$		n=6 hemiacetal

445
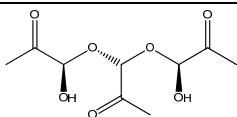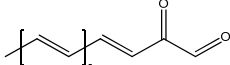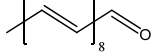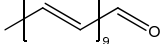
446 **Table 3.** Proposed peak assignments for Aerosol-CIMS mass spectra with I⁻ of atom-
447 ized solutions of 2 M formaldehyde/MG (1:1) in 3.1 M AS.

| m/z (amu) ± 1.0 amu	Ion Formula	Molecular Formula	Possible Structures	Mechanism
172.8	I⁻·CH_2O_2	CH_2O_2		Formic Acid
186.7	I⁻·$C_2H_4O_2$	$C_2H_4O_2$		cyclic F acetal
203.5	$C_5H_{11}O_6^-$·$2H_2O$	$C_5H_{12}O_6$		n=5 F hemiacetal
208.7	I⁻·CH_2O_2·$2H_2O$	CH_2O_2		Formic Acid
216.5	I⁻·$C_3H_6O_3$	$C_3H_6O_3$		Hydrated MG or cyclic F acetal
230.3	I⁻·$C_3H_4O_4$	$C_3H_4O_4$		n = 3 F hemiacetal
252.4	I⁻·$C_6H_6O_3$ I⁻·$C_3H_8O_4$·H_2O I⁻·$C_3H_6O_3$·$2H_2O$	$C_6H_6O_3$ $C_3H_8O_4$ $C_3H_6O_3$		MG aldol, n = 3 F hemiacetal, Hydrated MG, or cyclic F acetal
257.4	$C_8H_{17}O_9^-$	$C_8H_{18}O_9$		n=8 F hemiacetal
264.5	I⁻·$C_4H_{10}O_5$	$C_4H_{10}O_5$		n=4 F hemiacetal
272.2	I⁻·$C_6H_{10}O_4$	$C_6H_{10}O_4$		MG aldol and hemiacetal
	I⁻·$C_5H_6O_5$	$C_5H_6O_5$		MG + 2F hemiacetal
288.1	I⁻·$C_6H_{10}O_5$ I⁻·$C_6H_8O_4$·H_2O I⁻·$C_6H_6O_3$·$2H_2O$	$C_6H_{10}O_5$ $C_6H_8O_4$ $C_6H_6O_3$		MG aldol and hemiacetal
314.3	I⁻·$C_5H_{12}O_5$·$2H_2O$	$C_5H_{12}O_5$		MG + 2F hemiacetal
324.5	I⁻·$C_6H_{14}O_7$ I⁻·$C_6H_{12}O_6$·H_2O I⁻·$C_6H_{10}O_5$·$2H_2O$	$C_6H_{14}O_7$ $C_6H_{12}O_6$ $C_6H_{10}O_5$		n=6 F hemiacetal, MG hemiacetal
342.6	I⁻·$C_6H_{14}O_7$·H_2O I⁻·$C_6H_{12}O_6$·$2H_2O$	$C_6H_{14}O_7$ $C_6H_{12}O_6$		n=6 F hemiacetal, MG hemiacetal

448
449

18

Table 4. Proposed peak assignments for Aerosol-CIMS mass spectra with H_3O^+ of
atomized solutions of 0.5 M acetaldehyde/MG (1:1) in 3.1 M AS

m/z (amu) ± 1.0 amu	Ion Formula	Molecular Formula	Possible Structures	Mechanism
84.4	$CH_3O_2^+ \cdot 2H_2O$	CH_2O_2		Formic Acid
88.9	$C_3H_5O_3^+$	$C_3H_4O_3$		Pyruvic Acid
	$C_4H_7O^+ \cdot H_2O$ $C_4H_9O_2^+$	C_4H_6O $C_4H_8O_2$		A aldol
93.5	$C_2H_3O_3^+ \cdot H_2O$	$C_2H_2O_3$		Glyoxylic Acid
95.5	$C_2H_5O_3^+ \cdot H_2O$	$C_2H_4O_3$		Glycolic Acid
98.4	$C_2H_7O_2^+ \cdot 2H_2O$	$C_2H_6O_2$		Hydrated A
107.2	$C_3H_5O_3^+ \cdot H_2O$	$C_3H_4O_3$		Pyruvic Acid
	$C_4H_9O_2^+ \cdot H_2O$	$C_4H_8O_2$		A aldol
126.0	$C_7H_9O_2^+$	$C_7H_8O_2$		MG + 2 A aldol
134.0	$C_5H_{11}O_4^+ \cdot H_2O$	$C_5H_{10}O_4$		MG + A aldol
137.3	$C_5H_{11}O_3^+ \cdot H_2O$	$C_5H_{10}O_3$		Unknown
145.1	$C_6H_9O_4^+$ $C_6H_7O_3^+ \cdot H_2O$	$C_6H_8O_4$ $C_6H_6O_3$		MG aldol
162.9	$C_6H_{11}O_5^+$ $C_6H_9O_4^+ \cdot H_2O$	$C_6H_{10}O_5$ $C_6H_8O_4$		MG hemiacetal and aldol
164.7	$C_6H_{13}O_5^+$	$C_6H_{12}O_5$		MG aldol
	$C_6H_{11}O_4^+ \cdot H_2O$	$C_6H_{10}O_4$		MG hemiacetal and aldol
192.9	$C_{12}H_{15}O^+ \cdot H_2O$	$C_{12}H_{14}O$		6 A aldol
206.7	$C_{11}H_{11}O_4^+$	$C_{11}H_{10}O_4$		A + 3 MG aldol

235	$C_9H_{15}O_7^+$	$C_9H_{14}O_7$		MG hemiacetal
248.9	$C_{15}H_{17}O_2^+ \cdot H_2O$	$C_{15}H_{16}O_2$		1MG + 6 A aldol
289.6	$C_{18}H_{21}O^+ \cdot 2H_2O$	$C_{18}H_{20}O$		9 A aldol
297	$C_{20}H_{23}O^+ \cdot H_2O$	$C_{20}H_{22}O$		10 A Aldol

452

453

454 **Table 5.** Proposed peak assignments for Aerosol-CIMS mass spectra with I⁻ of atom-
455 ized solutions of 2 M acetaldehyde/MG (1:1) in 3.1 M AS.

| m/z (amu) ± 1.0 amu	Ion Formula	Molecular Formula	Possible Structures	Mechanism
172.7	$I^-\cdot CH_2O_2$ $I^-\cdot C_2H_6O$	CH_2O_2 C_2H_6O		Formic Acid
186.4	$I^-\cdot C_2H_4O_2$	$C_2H_4O_2$		Acetic Acid
189.6	$I^-\cdot C_2H_6O_2$	$C_2H_6O_2$		Hydrated A
194.6	$C_6H_9O_6^-$ $C_2H_7O_6S^-\cdot H_2O$	$C_6H_{10}O_6$ $C_2H_8O_6S$	Unknown	Unknown
208.4	$I^-\cdot CH_2O_2\cdot 2H_2O$	CH_2O_2		Formic Acid
216.3	$I^-\cdot C_3H_6O_3$	$C_3H_6O_3$		Hydrated MG
224.1	$I^-\cdot C_2H_6O_2\cdot 2H_2O$	$C_2H_6O_2$		Hydrated A
230.7	$I^-\cdot C_4H_8O_3$	$C_4H_8O_3$		A hemiacetal
	$I^-\cdot C_4H_6O_2\cdot H_2O$	$C_4H_6O_2$		Crotonic acid
242.9	$I^-\cdot C_5H_8O_3$	$C_5H_8O_3$		MG + A aldol
256.4	$I^-\cdot C_6H_{10}O_3$	$C_6H_{10}O_3$		MG aldol
264.4	$I^-\cdot C_4H_6O_3\cdot 2H_2O$	$C_4H_6O_3$		A hemiacetal
269.5	$I^-\cdot C_4H_{10}O_3\cdot 2H_2O$	$C_4H_{10}O_3$		A hemiacetal
272.2	$I^-\cdot C_6H_{10}O_4$	$C_6H_{10}O_4$		MG aldol and hemiacetal
342.3	$I^-\cdot C_6H_{12}O_6\cdot 2H_2O$	$C_6H_{12}O_6$		MG hemiacetal

456

457

458   *Figures*

459
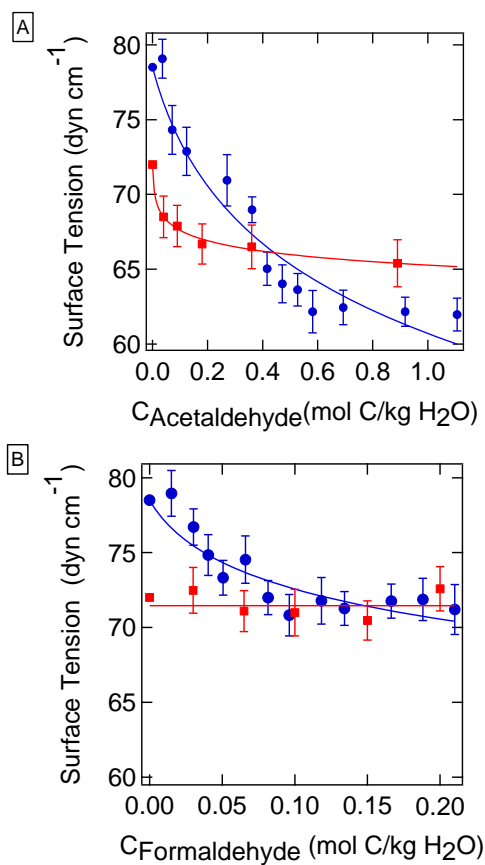
Figure 1. Surface tension of solutions containing (A) acetaldehyde and (B) formalde-

hyde in 3.1 M AS (●) and in water (■). The curves shown are fits to the data using the

Szyszkowski-Langmuir equation (Eq. (2)). A linear fit is shown for the formaldehyde-

water data as a guide to the eye.
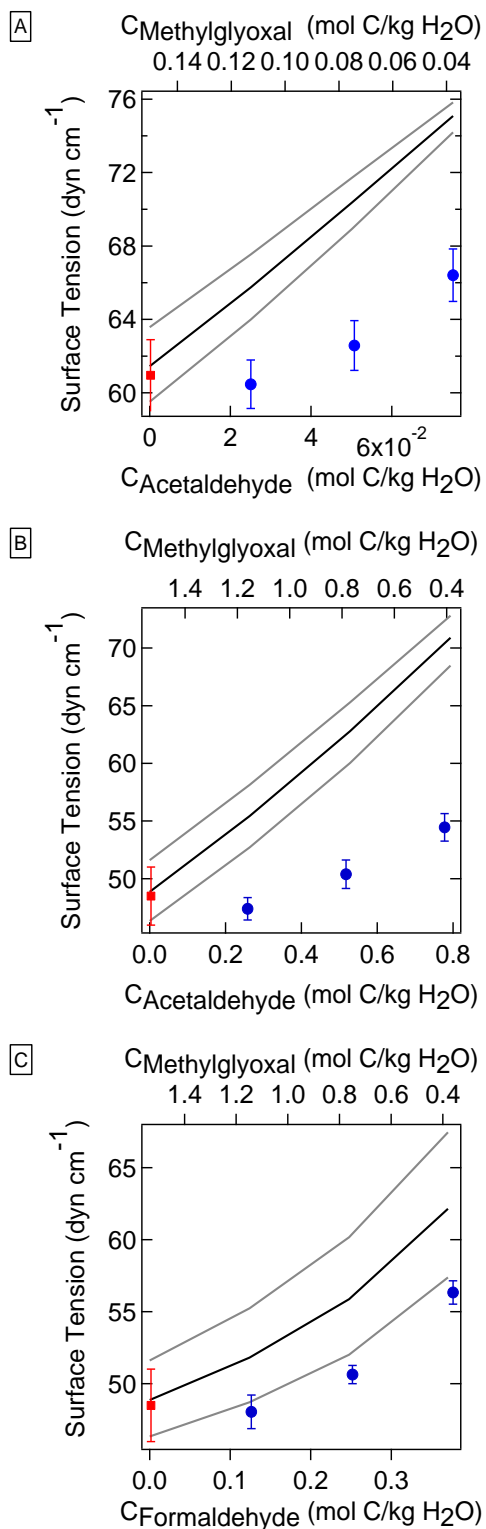
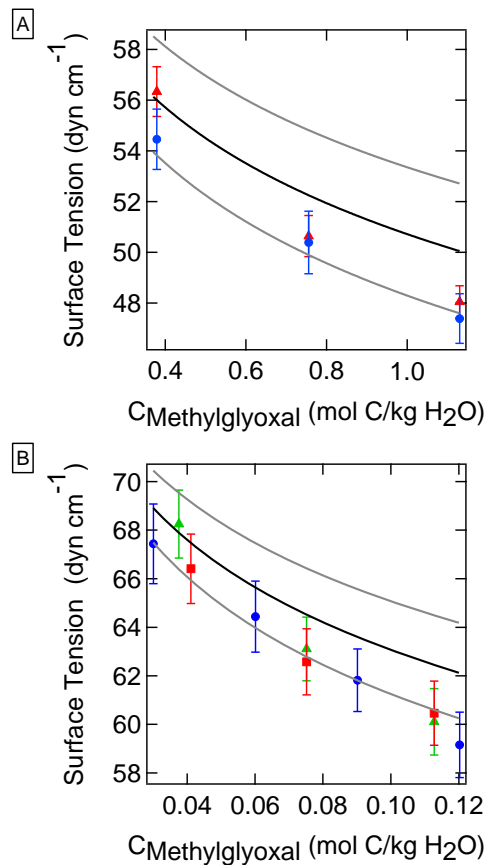**Figure 2**. Surface tension of binary mixtures of acetaldehyde or formaldehyde with

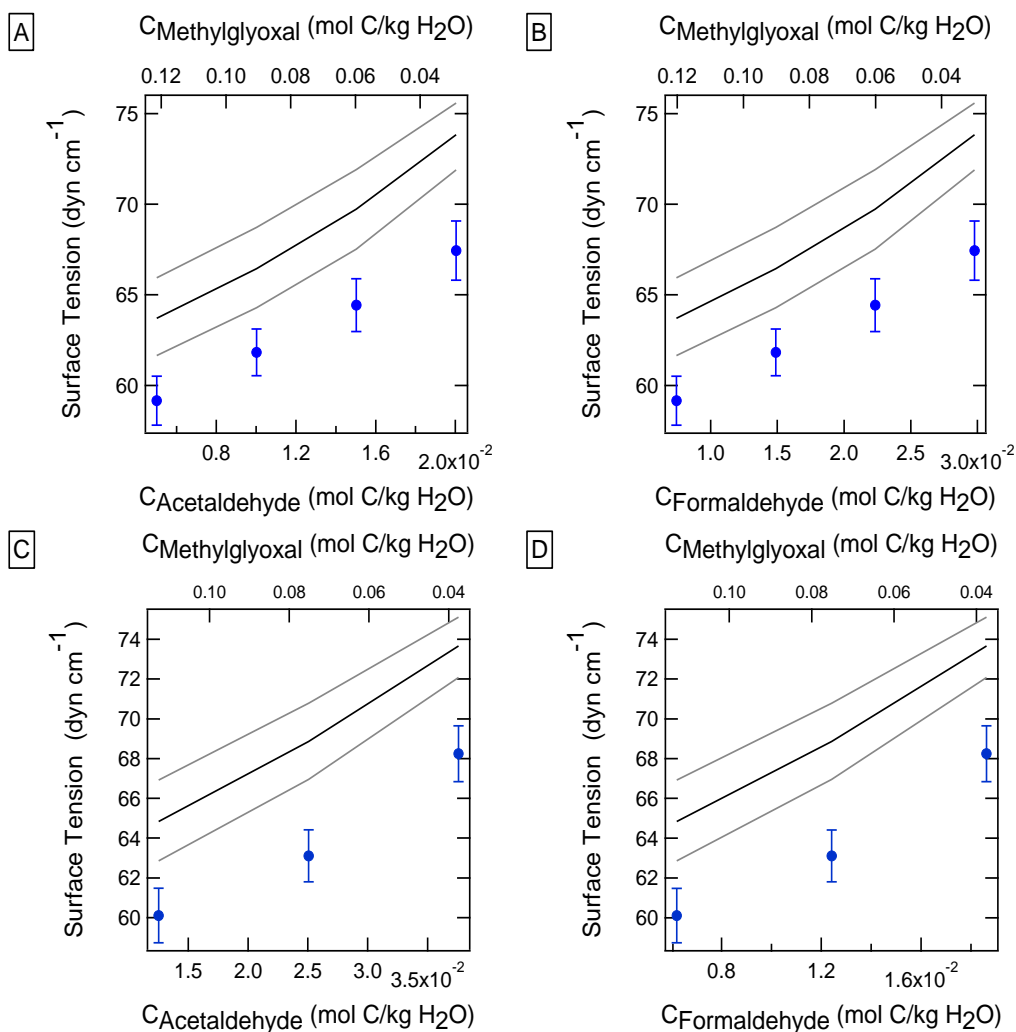MG in 3.1 M AS solutions. The total organic concentration was 0.05 M (A) or 0.5 M

469 (B, C). The black line shows Henning model predictions (Eq. (3)) using the parame-

470 ters listed in Table 1. The grey lines show the confidence interval of the model predic-

471 tions. ■: MG in AS (based on the Szyszkowski-Langmuir equation (Eq. (2)), using the

472 parameters in Table 1). ●: Acetaldehyde (A and B) or Formaldehyde (C) with MG in

473 3.1 M AS solutions.

474

Figure 3. Surface tension in binary and ternary organic mixtures (Fig 2 & 3) as a function of MG concentration. A) Binary mixtures (0.5 M total organic concentration) ▲: acetaldehyde-MG, ●: formaldehyde-MG B) 0.05 M total organic concentration. ▲: ternary mixture (acetaldehyde:formaldehyde=1:1 by mole, varying MG); ●: ternary mixture (acetaldehyde:formaldehyde=1:3 by mole, varying MG); ■: binary mixture (acetaldehyde-MG). Black curves indicate the Szyszkowski-Langmuir curve for MG in AS using the parameters in Table 1. Grey curves show the confidence intervals.

Figure 4. Surface tension data for ternary (acetaldehyde, formaldehyde and MG) mixtures in 3.1 M AS solutions. The molar ratios of acetaldehyde to formaldehyde are 1:3 (A and B) and 1:1 (C and D). The total organic concentration was constant at 0.05 M. The black line shows Henning model predictions using the parameters listed in Table 1. The grey lines show the confidence interval of the predicted data.
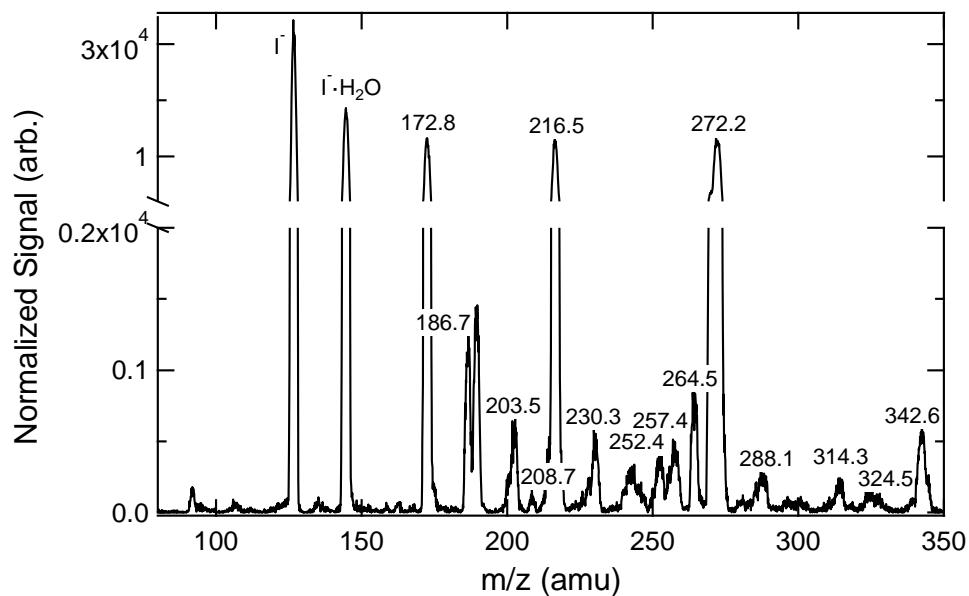
495
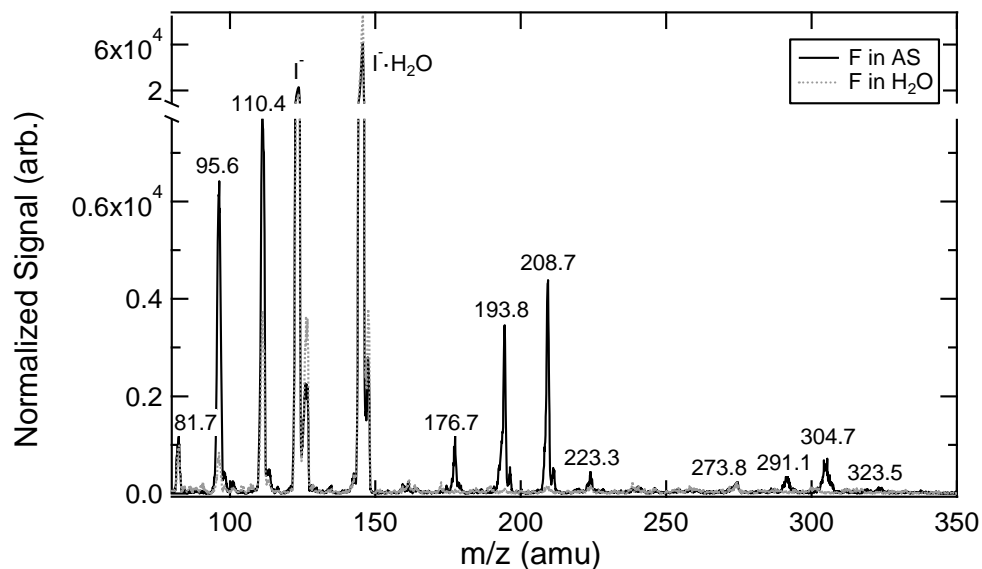
Figure 5. Aerosol-CIMS spectra of atomized solutions of 0.2 M formaldehyde in 3.1

M AS and H_2O. See the text for details of sample preparation and analysis. Negative-

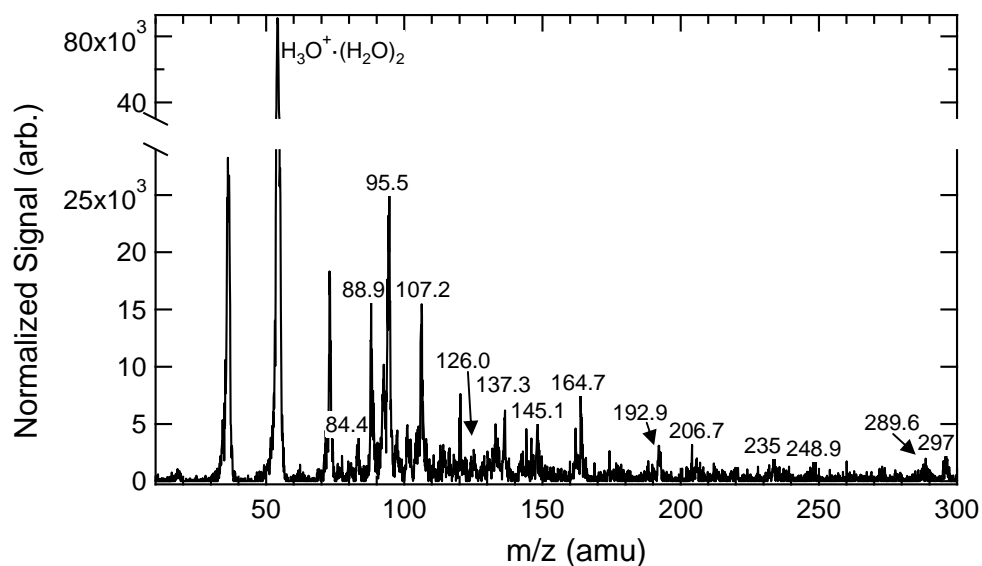ion mass spectrum obtained using I^- as the reagent ion.

499

500

Figure 6. Aerosol-CIMS spectra of atomized solutions of 2 M formaldehyde/MG

(1:1) in 3.1 M AS. See the text for details of sample preparation and analysis. Nega-

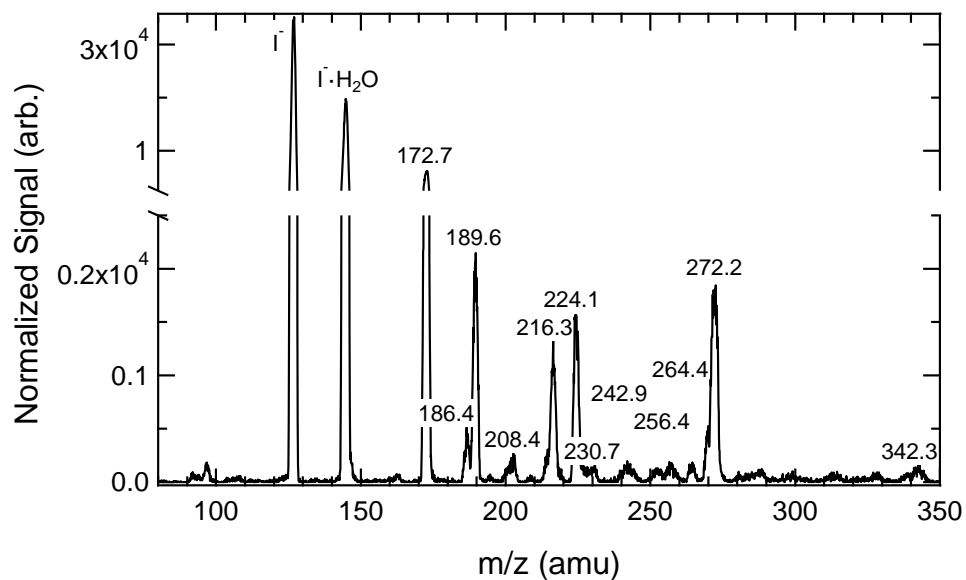tive-ion mass spectrum obtained using I^- as the reagent ion.

504

505

Figure 7. Aerosol-CIMS spectra of atomized solutions of 0.5 M acetaldehyde/MG

(1:1) in 3.1 M AS. See the text for details of sample preparation and analysis. Posi-

tive-ion mass spectrum using $H_3O^+\cdot(H_2O)_n$ as the reagent ion.

509

510

Figure 8. Aerosol-CIMS spectra of atomized solutions of 2 M acetaldehyde/MG (1:1)

in 3.1 M AS. See the text for details of sample preparation and analysis. Negative-ion

mass spectrum was obtained using I^- as the reagent ion.

514

Supporting Information

Reactive processing of formaldehyde and acetaldehyde in aqueous aerosol mimics: Surface tension depression and secondary organic products

Zhi Li, Allison N. Schwier, Neha Sareen, V. Faye McNeill*

Department of Chemical Engineering, Columbia University, New York, NY, 10027, USA

* To whom correspondence should be addressed. Email: vfm2103@columbia.edu

7 pages, 4 tables, 3 figures

Table S1. Calculated errors between the Henning model predictions (using eq. (3)) and experimentally measured surface tension values.

Total Organic Concentration	Species	MG[*]	Acet[*]	Form[*]	Model Prediction	Measured Data	Error
(mol/L)		(mol C/kg H$_2$O)			(dyn cm^{-1})		(%)
0.05	MG Acet:Form=1:3	0.030	0.020	0.030	73.848	67.438	8.680
		0.060	0.015	0.022	69.730	64.438	7.589
		0.090	0.010	0.015	66.454	61.822	6.970
		0.120	0.005	0.007	63.712	59.159	7.146
	MG Acet:Form=1:1	0.113	0.013	0.006	64.832	60.105	7.292
		0.075	0.025	0.012	68.868	63.105	8.368
		0.038	0.038	0.019	73.673	68.249	7.362
	MG/Acet	0.038	0.075	N/A	75.081	66.407	11.553
		0.075	0.051	N/A	70.361	62.575	11.066
		0.113	0.025	N/A	65.746	60.465	8.032
0.5	MG/Acet	1.153	0.259	N/A	55.433	47.388	14.512
		0.770	0.518	N/A	62.788	50.389	19.747
		0.385	0.778	N/A	70.895	54.454	23.190
	MG/Form	1.148	N/A	0.126	51.809	48.046	7.263
		0.763	N/A	0.252	55.868	50.638	9.361
		0.381	N/A	0.377	62.142	56.334	9.346

[*]MG: Methylglyoxal; Acet: Acetaldehyde; Form: Formaldehyde

Density functional theory calculations of paraformaldehyde ionization by I⁻

Density functional theory calculations were used to evaluate the thermodynamic favorability of the following chemical ionization reaction for paraformaldehyde (n = 9):

$$I^- + R{-}OH \rightarrow R\text{-}O^- + HI \tag{S1}$$

Geometry optimizations and energy calculations were performed using Jaguar 7.7 (Schrödinger, Inc.). The B3LYP functional was used with the ERMLER2 basis set, which allows the treatment of iodine via the use of effective core potentials (Lajohn et al., 1987). The results of the calculation are shown in Table S2. We found that reaction S1 is thermodynamically favorable, with ΔG = -4.99 kJ mol^{-1}. We believe that the ionized species is stabilized by interactions between the ionized ─O⁻ and the other terminal hydroxyl group(s) on the molecule (see the optimized geometry in Figure S1).

Table S2. Calculated total Gibbs free energy.

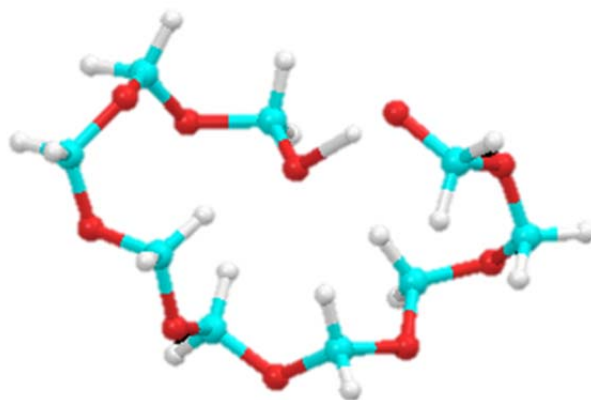| Species	Gtot (Hartrees)
I-	-111.5214881
Paraformaldehyde (n= 9)	-1106.4844260
Ionized paraformaldehyde (n = 9)	-1105.9625590
HI	-112.0452540

Figure S1. Optimized structure of ionized paraformaldehyde (n = 9). White = H, red = O, cyan = C.

Table S3. Proposed peak assignments for Aerosol-CIMS mass spectra with H_3O^+ of atomized solutions of 1 M formaldehyde in 3.1 M AS.

m/z (amu) ± 1.0 amu	Ion Formula	Molecular Formula	Possible Structures	Mechanism
77.2	$C_2H_5O_3^+$	$C_2H_4O_3$		hemiacetal
94.9	$C_2H_5O_3^+\cdot H_2O$	$C_2H_4O_3$		hemiacetal
	$C_2H_7O_4^+$	$C_2H_6O_4$		
107	$C_3H_7O_4^+$	$C_3H_6O_4$		hemiacetal
113.2	$C_2H_5O_3^+\cdot 2H_2O$	$C_2H_4O_3$		hemiacetal
	$C_2H_7O_4^+\cdot H_2O$	$C_2H_6O_4$		
124.9	$C_3H_7O_4^+\cdot H_2O$ $C_3H_9O_5^+$	$C_3H_6O_4$ $C_3H_8O_5$		hemiacetal
137	$C_4H_9O_5^+$	$C_4H_8O_5$		hemiacetal
143.5	$C_3H_7O_4^+\cdot 2H_2O$ $C_3H_9O_5^+\cdot H_2O$	$C_3H_6O_4$ $C_3H_8O_5$		hemiacetal

Table S4. Proposed peak assignments for Aerosol-CIMS mass spectra with H_3O^+ of atomized solutions of 0.5 M formaldehyde/MG (1:1) in 3.1 M AS.

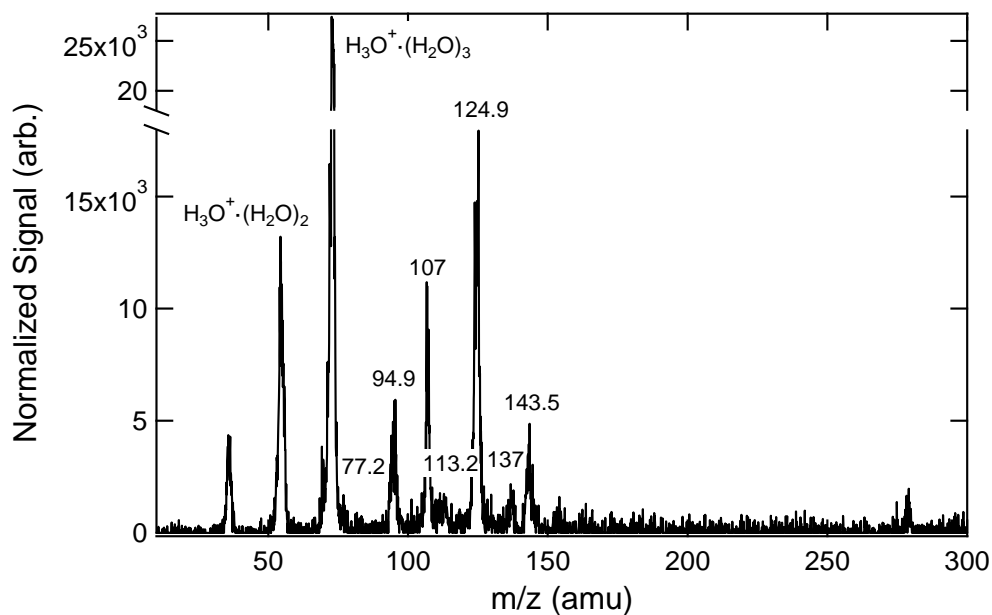| m/z (amu) ± 1.0 amu	Ion Formula	Molecular Formula	Possible Structures	Mechanism
84.3	$CH_3O_2^+\cdot 2H_2O$	CH_2O_2		Formic Acid
	$CH_5O_2^+\cdot 2H_2O$	CH_4O_2		Hydrated F
96.1	$C_2H_5O_3^+\cdot H_2O$	$C_2H_4O_3$		hemiacetal
125.1	$C_3H_7O_4^+\cdot H_2O$	$C_3H_6O_4$		hemiacetal
154.9	$C_4H_9O_5^+\cdot H_2O$	$C_4H_8O_5$		n=4 hemiacetal

Figure S2. Aerosol CIMS spectra of atomized solutions of 1 M formaldehyde in 3.1 M AS. See the text for details of sample preparation and analysis. Positive-ion mass spectrum obtained using $H_3O^+\cdot(H_2O)_n$ as the reagent ion.
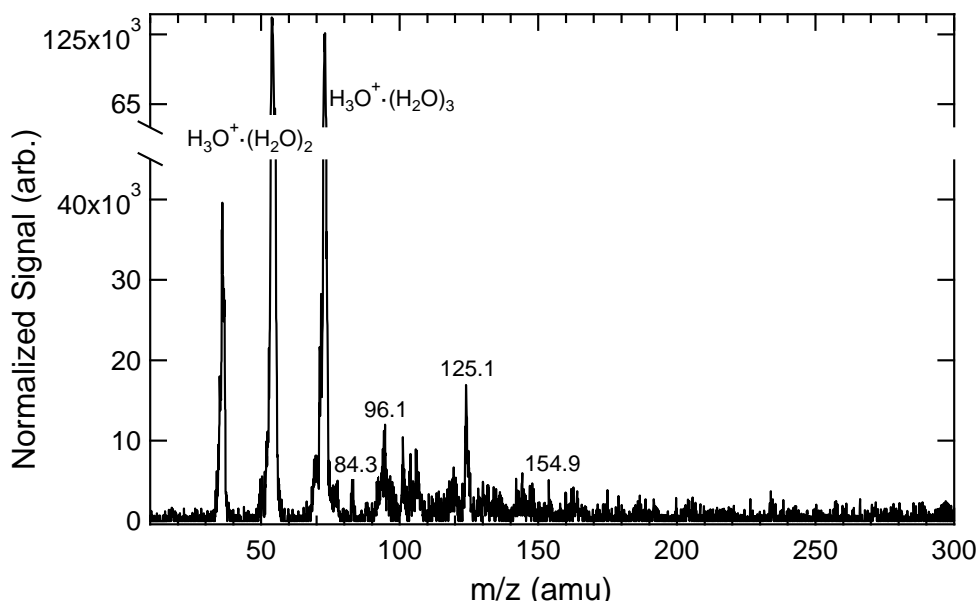

Figure S3. Aerosol CIMS spectra of atomized solutions of 0.5 M formaldehyde/MG (1:1) in 3.1 M AS. See the text for details of sample preparation and analysis. Positive-ion mass spectrum with $H_3O^+\cdot(H_2O)_n$ as the reagent ion.

Predictions of paraformaldehyde sulfate ester production

We attribute the signal at 193.8 amu in the formaldehyde/AS spectrum to the formaldehyde hemiacetal dimer ($C_2H_6O_6S$). After 24 h of reaction, the mass spectrum shows signal of 3500 counts/s at this mass. Assuming an upper bound sensitivity of 100 counts s^{-1} ppt^{-1} for this species (Sareen et al., 2010), and based on the volume weighted geometric mean diameter of 414($\pm$14) nm and the average particle concentration of $\sim$4$\times$10^4 cm^{-3}, we estimate a lower limit for the in-particle concentration of this species to be $\sim$10^{-3} M. Taking into account the concentrating effect of aerosol dehydration after atomization and dilution of the aerosol stream with dry N_2, we infer a $C_2H_6O_6S$ concentration of $\geq$2$\times$10^{-4} M in the bulk solution after 24 h of reaction.

According to Deno and Newman the formation of alcohol ester sulfates occurs via the reaction with H_2SO_4 even if SO_4^{-2} and HSO_4^- are present (Deno and Newman, 1950). We assume here that the same is true for the formation of $C_2H_6O_6S$ from $C_2H_6O_3$. Minerath and coworkers reported that sulfate esterification of ethylene glycol, a close structural analog of $C_2H_6O_3$, occurred in 75 wt% H_2SO_4 according to:

$$C_2H_6O_2 + H_2SO_4 \leftrightarrow C_2H_6O_5S + H_2O \tag{S2}$$

with a forward pseudo-first-order rate constant of 7.30$\times$10^{-4} s^{-1} and reverse pseudo-first-order rate constant of 3.00$\times$10^{-4} s^{-1} (Minerath et al., 2008). This translates to a forward second-order rate constant of 6.29$\times$10^{-5} $M^{-1}s^{-1}$ and reverse second-order rate constant of 1.43$\times$10^{-5} $M^{-1}s^{-1}$.

The following reaction was modeled using POLYMATH 6.10:

$$2\ HCHO\ (+H_2O) \rightarrow C_2H_6O_3 \tag{S3}$$

$$C_2H_6O_3 + H_2SO_4 \leftrightarrow C_2H_6O_5S + H_2O \tag{S4}$$

With k_{S4} = 6.29$\times$10^{-5} $M^{-1}s^{-1}$ and k_{-S4} = 1.43$\times$10^{-5} $M^{-1}s^{-1}$. Formaldehyde dimerization is assumed to be fast, with a rate constant similar to glyoxal dimerization (pseudo first-order rate constant = 5$\times$10^{-4} s^{-1} (Fratzke and Reilly, 1986)). We found that the model was insensitive to this parameter, because reaction (S4) was rate-limiting. Based on this model we predict a maximum $C_2H_6O_5S$ concentration of $\sim$7$\times$10^{-8} M after 24 h of reaction. This calculation provides an upper bound estimate of $C_2H_6O_5S$ concentration since other sinks for formaldehyde monomer and $C_2H_6O_3$ exist in the system which are not represented by this simple model. Nevertheless, this model underpredicts the observed $C_2H_6O_6S$ concentration by a factor of $\geq$3000.

REFERENCES

Deno, N. C. and Newman, M. S.: Mechanism of Sulfation of Alcohols, *J. Am. Chem. Soc.*, *72* (9), 3852-3856, 1950.

Fratzke, A. R. and Reilly, P. J.: Thermodynamic and Kinetic Analysis of the Dimerization of Aqueous Glyoxal, *Int. J. Chem. Kinetics*, *18,* 775-789, 1986.

Lajohn, L. A., Christiansen, P. A., Ross, R. B., Atashroo, T., and Ermler, W. C.: Abinitio Relativistic Effective Potentials with Spin Orbit Operators .3. Rb Through Xe, *J. Chem. Phys.*, *87* (5), 2812-2824, 1987.

Minerath, E. C., Casale, M. T., and Elrod, M. J.: Kinetics feasibility study of alcohol sulfate esterification reactions in tropospheric aerosols, *Environ. Sci. Technol.*, *42* (12), 4410-4415, 2008.

Sareen, N., Schwier, A. N., Shapiro, E. L., Mitroo, D. M., and McNeill, V. F.: Secondary organic material formed by methylglyoxal in aqueous aerosol mimics, *Atmos. Chem. Phys.*, *10*, 997-1016, 2010.